Temporal Raphe Sign in Elderly Patients With Large Optic Disc Cupping: Its Evaluation as a Predictive Factor for Glaucoma Conversion

AHNUL HA, YOUNG KOOK KIM, JIN-SOO KIM, JIN WOOK JEOUNG, AND KI HO PARK

• PURPOSE: To determine baseline clinical features associated with conversion to glaucoma in elderly patients with large optic-disc cupping.
• DESIGN: Retrospective cohort study.
• METHODS: Seventy-two eyes of 72 untreated elderly (≥65-year-old) patients with large vertical cup-to-disc ratio (CDR ≥0.7) and without any other glaucomatous findings were included. They had undergone a full ophthalmologic examination twice per year for at least 5 years. The optic nerve head (ONH), peripapillary retinal nerve fiber layer (RNFL), and macular ganglion cell–inner plexiform layer (GCIPL) were imaged with Cirrus high-definition optical coherence tomography (OCT). Presence of temporal raphe sign on the OCT's GCIPL thickness map was assessed as one of the morphologic factors. Conversion to normal-tension glaucoma (NTG) was defined as structural or functional deterioration on either red-free RNFL photography or standard automated perimetry, respectively. The utility of the baseline factors associated with conversion to NTG were identified.
• RESULTS: During the 5.5-year follow-up, 19 eyes (26.4%) converted to NTG. There were no significant differences in demographics, systemic factors, intraocular pressure factors, or OCT parameters between the nonconverters and converters. Interestingly, the temporal raphe sign was observed in the converters (18/19, 94.7%) much more frequently than in the nonconverters (3/53, 5.7%, $P < .001$) at baseline. A Cox proportional hazards model indicated the significant influences of temporal raphe sign positivity (hazard ratio 6.823, 95% confidence interval 2.574, 18.088, $P < .001$) on conversion to NTG.
• CONCLUSIONS: In elderly subjects with large CDR, temporal raphe sign positivity on the baseline macular GCIPL thickness map was associated with faster conversion to NTG. (Am J Ophthalmol 2020;219:205–214.

Accepted for publication Jul 1, 2020.

Department of Ophthalmology, Jeju National University Hospital (A.H.), Jeju-si, Republic of Korea; Department of Ophthalmology, Seoul National University College of Medicine (A.H., Y.K.K., J.-S.K., J.W.J., K.H.P.), Seoul, Republic of Korea; Department of Ophthalmology, Seoul National University Hospital (Y.K.K., J.W.J., K.H.P.), Seoul, Republic of Korea; Department of Ophthalmology, Chungnam National University Sejong Hospital (J.-S.K.), Sejong, Republic of Korea.

Inquiries to Ki Ho Park, Department of Ophthalmology, Seoul National University Hospital, Seoul National University College of Medicine, 101 Daehak-ro, Jongno-gu, Seoul 03080, Republic of Korea; e-mail: kihopark@snu.ac.kr

THE OPTIC NERVE HEAD (ONH) AND THE RETINAL nerve fiber layer (RNFL) are sensitive indicators for prediction of early-glaucomatous damage. However, they are also subject to age-related wear and tear; in fact, several histologic studies on retinal ganglion cell (RGC) axons of the optic nerve or RGC cells in the retina have shown steady loss of cells with age.[1–3] Similarly, previous studies based on optical coherence tomography (OCT) measurement have reported that circumpapillary RNFL thickness systematically becomes thinner with age.[4–8] Additionally, the spatial patterns of structural alterations in aging and glaucoma have been reported to be similar.[9–11] A series of OCT studies in healthy eyes have demonstrated cross-sectional age effects of minimum rim width, and the circumpapillary RNFL thickness is greatest within the inferior and inferior temporal sectors.[12–14] This similarity in the pattern of optic nerve damage in glaucoma patients and normal controls suggests that there may be an age-related pattern of regional susceptibility in the optic nerve comprising neuronal or nonneuronal structural components, or both.

Among all glaucoma suspects, therefore, elderly eyes showing ONH features that are suspicious or suggestive of early glaucoma are probably among the greatest challenges for clinicians. Age-related optic nerve damage commonly creates the impression of a shallow form of optic disc cupping.[15] Since aged connective tissues are most commonly stiffer than younger connective tissues,[16–18] the aged lamina may be less likely to deform posteriorly. Likewise, shallower cupping is frequent in eyes with normal-tension glaucoma (NTG).[19,20] Although the magnitude of intraocular pressure (IOP)–related stress for a given level of IOP is determined by the 3-dimensional anatomy of the eye, low IOP level generally is less likely to cause posterior deformation of the ONH tissues. In addition, both glaucoma and aging are commonly accompanied by peripapillary atrophy.[21–24] In eyes manifesting increased ONH cupping with normal IOP and no other glaucomatous findings, therefore, it can be especially challenging to determine which cases will go on to progress at rates that exceed age effects.

0002-9394/$36.00
https://doi.org/10.1016/j.ajo.2020.07.001

Because of the strict superior/inferior segregation of the temporal RNFL across the horizontal raphe, glaucomatous damages are often asymmetric across the horizontal meridian, especially in the early stage.[25–27] Recently, our group explored the glaucoma-diagnostic ability of a steplike configuration near the temporal raphe on the Cirrus high-definition optical coherence tomography (HD-OCT) macular ganglion cell–inner plexiform layer (GCIPL) thickness map (the so-called temporal raphe sign).[28] The temporal raphe sign was proved to be useful for discrimination of preperimetric glaucoma cases,[28] highly myopic eyes with glaucomatous damage,[29] and GCIPL thinning due to glaucoma compared with nonglaucomatous optic neuropathy.[30] In the present study, Korean elderly patients showing a large cup-to-disc ratio (CDR) but no other glaucomatous findings were followed up for an average of 5.5 years, and their baseline clinical factors (including temporal raphe sign positivity) associated with early glaucomatous progression were analyzed.

METHODS

• **STUDY SUBJECTS:** This retrospective cohort study enrolled eligible-patient data from the Clinical Data Warehouse of Seoul National University Hospital Patients Research Environment (CDW SUPREME, compiled from January 2010 to December 2018). These electronic medical records of elderly patients (aged 65 years or older) who had visited glaucoma clinics of Seoul National University Hospital for regular checkups were retrospectively reviewed. The study was approved by the Institutional Review Board of Seoul National University Hospital, and fully adhered to the Declaration of Helsinki. Informed consent was waived because of the study's retrospective nature.

The current study was conducted to establish appropriate treatment strategies for elderly patients with either early glaucoma or glaucoma suspect. Each subject underwent a complete ophthalmic examination: a visual acuity assessment, refraction, slit-lamp biomicroscopy, gonioscopy, Goldmann applanation tonometry (GAT; Haag-Streit, Koniz, Switzerland), and dilated-funduscopic examination. Additionally, they underwent the following: central corneal thickness measurement (Orbscan 73 II; Bausch & Lomb Surgical, Rochester, New York, USA), axial length (AXL) measurement (Axis II PR; Quantel Medical, Inc, Bozeman, Montana, USA), digital color stereo disc photography, red-free RNFL photography, Cirrus spectral-domain (SD) OCT (Carl Zeiss Meditec, Dublin, California, USA) scanning, and Humphrey visual field (VF) central 24-2 threshold tests (HFA II; Humphrey Instruments Inc, Dublin, California, USA).

The elderly patients who were enrolled showed large CDR without any other findings related to glaucoma. The specific inclusion criteria were as follows: (1) vertical CDR greater than 0.7; (2) open anterior chamber angles; (3) normal untreated IOP level (≤21 mm Hg); (4) no focal RNFL change (as visible on red-free RNFL images); (5) normal VF with the Glaucoma Hemifield Test and mean deviation within normal limits; (6) a follow-up duration longer than 5 years. To determination CDR, stereo disc photographs were independently evaluated by 2 glaucoma specialists (A.H., J.S.K.), and cases were included only if both evaluators assessed vertical CDR greater than 0.7.

Patients were excluded for 1 or more of the following reasons: best-corrected visual acuity below 20/40; unreliable VF examination based on the reliability indices (fixation loss rate >20%, false-positive and false-negative error rates >25%); any posterior-pole lesions possibly affecting VF examination results; and history of intraocular surgery (excluding uncomplicated cataract surgery) at baseline or during the follow-up period. If both eyes were qualified based on the inclusion criteria, one eye was randomly selected for further analysis.

• **CIRRUS HD-OCT MEASUREMENT:** Optic-disc (optic disc cube 200 × 200 protocol) and macular scans (macular cube, 512 × 128 protocol) using HD-OCT software (Cirrus, version 6.0; Carl Zeiss Meditec) for RNFL and macula GCIPL thickness measurements, respectively, were carried out. The included RNFL parameters were average thickness (360° measure), 4-quadrant thickness (temporal, superior, nasal, and inferior), and thickness at each of the 12 clock-hour sectors. The ONH parameters that were analyzed were the disc area, rim area, average CDR, vertical CDR, and cup volume. The evaluated macular GCIPL indices were the average, minimum, and 6 sectoral thicknesses (superotemporal, superior, superonasal, inferonasal, inferior, inferotemporal). Only high-quality scans (signal strength ≥7, absence of discontinuity or misalignment, no involuntary saccade, blinking artifacts, segmentation failure, or artifacts) were applied to the final analysis.

• **ESTIMATION OF CORRECTED OPTIC DISC AREA:** The measured size of a feature in the fundus is dependent on the magnification of the camera and magnification of the optical system of the eye.[31] Thus, the corrected disc areas were obtained by substituting the subject's AXL, taking into account the magnification factors related to the SD-OCT camera and the eye.[32] The formula for optic disc area correction was as follows: Corrected optic disc area = $3.382^2 \times 0.01306^2 \times (\text{AXL}-1.82)^2 \times$ (Computed SD-OCT optic disc area).[33]

• **DETERMINATION OF TEMPORAL RAPHE SIGN:** In this study, the GCIPL hemifield test with a MATLAB-based (MathWorks Inc, Natick, Massachusetts, USA) computer program was employed to determine temporal raphe sign positivity. For details on this program, the reader can access a previously published paper.[28,29] In brief, the GCIPL

TABLE 1. Comparison of Baseline Demographics and Clinical Variables Between Converters and Nonconverters

	Converters (n = 19)	Nonconverters (n = 53)	*P*
Demographic data			
Age (years)	72.8 ± 4.3	73.1 ± 5.2	.823[a]
Sex (male/female)	11/8	23/30	.277[b]
Diabetes mellitus (yes/no)	7/12	21/32	.831[b]
Hypertension (yes/no)	9/10	25/28	.988[b]
Pulmonary disease (yes/no)	4/13	10/35	.913[b]
Heart disease (yes/no)	5/11	16/27	.671[b]
Clinical data			
Intraocular pressure (mm Hg)			
Baseline	15.4 ± 3.5	15.8 ± 4.0	.701[a]
Mean	15.2 ± 1.7	15.5 ± 1.5	.473[a]
Long-term fluctuation	2.7 ± 1.2	2.1 ± 1.5	.121[a]
Follow-up peak	18.5 ± 4.2	17.1 ± 3.9	.193[a]
Central corneal thickness (μm)	523.8 ± 41.5	530.5 ± 47.1	.585[a]
Axial length (mm)	24.8 ± 1.7	24.1 ± 2.1	.196[a]
Follow-up duration (y)	5.6 ± 0.7	5.4 ± 0.9	.384[a]

[a]Student *t* test.
[b]Chi-square test.

Hemifield Test automatically extracted from the macular GCIPL thickness map, a 32-bit color-scale image of an elliptical annulus having a 2.0-mm vertical outer radius and a 2.4-mm horizontal outer radius. Then, automated image processing was conducted for line detection. Ultimately, the GCIPL Hemifield Test result was deemed positive (ie, "temporal raphe sign positivity") if the following 3 conditions were met: (1) continuous detection of the reference line (a horizontal line dividing the superior and inferior hemifields) for longer than one-half of the distance between the temporal inner elliptical annulus and the outer elliptical annulus; (2) an average GCIPL thickness difference within 10 pixels of the reference line, both above and below, of ≥5 μm; and (3) an average RGB color range for those 10 pixels above and below the reference line showing blue in 1 hemifield and red/yellow/white in the other one.

• **DISCRIMINATION OF GLAUCOMA CONVERSION:** Conversion to NTG was defined as glaucomatous progression to the point of meeting NTG criteria. That is, development of focal RNFL defect attributable to glaucoma (the structural endpoint) and/or reproducible glaucomatous VF abnormalities (the functional endpoint). The functional endpoint was reached when 1 or more of the Anderson and Patella criteria were met: (1) a cluster of 3 points located in typical glaucomatous areas on the pattern deviation plot, which points showed a $P < .05$ and at least 1 point with $P < .01$, none of which could be edge points unless it was located either immediately above or immediately below the nasal horizontal meridian; (2) Pattern standard deviation < 5%; or (3) glaucoma hemifield test result outside the normal limits. A confirmed VF defect required 2 consecutive, abnormal VF test results showing VF damage in the same test locations. Each study eye was evaluated whether the structural and/or functional endpoint was reached independently by 2 experts' (A.H. and Y.K.K.) masked grading. If the opinions of the 2 examiners on progression differed, consensus was reached post discussion. And if no consensus could be reached, that eye was excluded from subsequent analysis. The confirmation that the endpoint was attributable to NTG with exclusion of the possibility of artifacts as the cause of RNFL or VF abnormality was made after masked clinical chart review by a third masked evaluator (K.H.P.).

• **STATISTICAL ANALYSIS:** The independent Student *t* test was used to compare the normally distributed data, and the χ^2 test was used to analyze the categoric data. The intergroup cumulative risk ratios for structural and functional progression were compared by Kaplan-Meier survival analysis and log-rank test. The endpoint time was defined, for patients showing conversion, as the time of NTG diagnosis, and for nonconverters, as the time of the final follow-up visit. The hazard ratios for the associations among the potential risk factors (age, sex, systemic factors, central corneal thickness, AXL, presence of optic disc hemorrhage, IOP parameters, functional parameters from standard automated perimetry, structural indices on OCT RNFL/ONH/ganglion cell analysis, and presence of temporal raphe sign) and glaucoma progression were determined by Cox proportional hazards modeling. For each factor, a univariate analysis was performed, and those showing

TABLE 2. Comparison of Baseline Variables Between Converters and Nonconverters

	Converters (n = 19)	Nonconverters (n = 53)	*P*
Standard automated perimetry			
MD (dB)	−1.08 ± 1.40	−1.05 ± 1.55	.940[a]
PSD (dB)	1.77 ± 0.41	1.75 ± 0.38	.830[a]
Number of points with $P < 5\%$	3.26 ± 1.33	3.04 ± 1.48	.561[a]
Number of points with $P < 1\%$	1.10 ± 1.59	1.04 ± 1.45	.866[a]
Visual field index (%)	98.7 ± 1.15	98.9 ± 1.02	.507[a]
RNFL and ONH analysis			
RNFL thickness (μm)			
Average	84.2 ± 12.4	82.1 ± 11.9	.524[a]
Quadrant			
Superior	101.5 ± 15.9	100.2 ± 18.1	.771[a]
Temporal	61.1 ± 5.16	64.0 ± 8.22	.146[a]
Inferior	102.3 ± 23.7	100.1 ± 24.2	.720[a]
Nasal	64.8 ± 12.4	64.8 ± 10.1	.917[a]
Rim area (mm^2)[b]	1.01 ± 0.16	0.99 ± 0.18	.684[a]
Disc area (mm^2)[b]	2.47 ± 0.38	2.50 ± 0.32	.740[a]
Cup-to-disc ratio			
Average	0.77 ± 0.08	0.78 ± 0.09	.671[a]
Vertical	0.73 ± 0.05	0.74 ± 0.08	.612[a]
Cup volume (mm^3)	0.51 ± 0.17	0.55 ± 0.18	.398[a]
Macular ganglion cell analysis			
Temporal raphe sign (yes/no)	18/1	3/50	< .001[c]
GCIPL thickness (μm)			
Average	72.8 ± 4.46	72.2 ± 5.53	.653[a]
Minimum	66.7 ± 7.06	65.9 ± 7.01	.680[a]
Sector			
Superotemporal	73.2 ± 4.98	71.4 ± 5.33	.218[a]
Superior	71.0 ± 6.81	70.9 ± 6.66	.967[a]
Superonasal	77.0 ± 5.85	75.6 ± 5.39	.360[a]
Inferior	70.1 ± 6.27	69.0 ± 6.49	.523[a]
Inferotemporal	71.9 ± 8.01	71.5 ± 8.03	.846[a]
Inferonasal	73.8 ± 5.30	73.3 ± 7.24	.783[a]

GCIPL = ganglion cell–inner plexiform layer; MD = mean deviation; ONH = optic nerve head; PSD = pattern standard deviation; RNFL = retinal nerve fiber layer.

[a]Student *t* test.

[b]Corrected area = $3.382^2 \times 0.01306^2 \times (\text{axial length}-1.82)^2 \times$ (computed SD-OCT area).

[c]Chi-square test.

a value of $P < .1$ were included in the subsequent multivariate model. The adjusted hazard ratios with 95% confidence intervals were calculated. All of the statistical analyses were performed using the SPSS statistical package (SPSS 22.0; SPSS, Chicago, Illinois, USA). The data ranges were recorded as mean ± standard deviations; the criterion for statistical significance was a 2-sided *P* value less than .05.

RESULTS

INITIALLY, 93 EYES MEETING THE ELIGIBILITY CRITERIA WERE included. Among them, 16 were excluded because of missing data. Another 5 were excluded owing to associated retinal disease diagnosed during the follow-up, which left a total of 72 eyes of 72 patients.

Of the 72 eyes, 19 (26.4%) achieved endpoints for NTG and 53 (73.6%) did not, by the point of the final analysis (December 2018). Among the 19 eyes showing conversion to glaucoma, 12 reached the structural endpoint and 6 reached the functional endpoint. One patient reached both structural and functional endpoints. The mean follow-up time was 5.6 ± 0.7 years for converters and 5.4 ± 0.9 years for nonconverters. The mean conversion time for the converter group was 3.5 ± 1.4 years.

The average RNFL thickness slope was greater for converters than for nonconverters (−0.76 ± 0.58 vs −0.24 ± 0.31, $P < .001$). The average GCIPL thickness slope

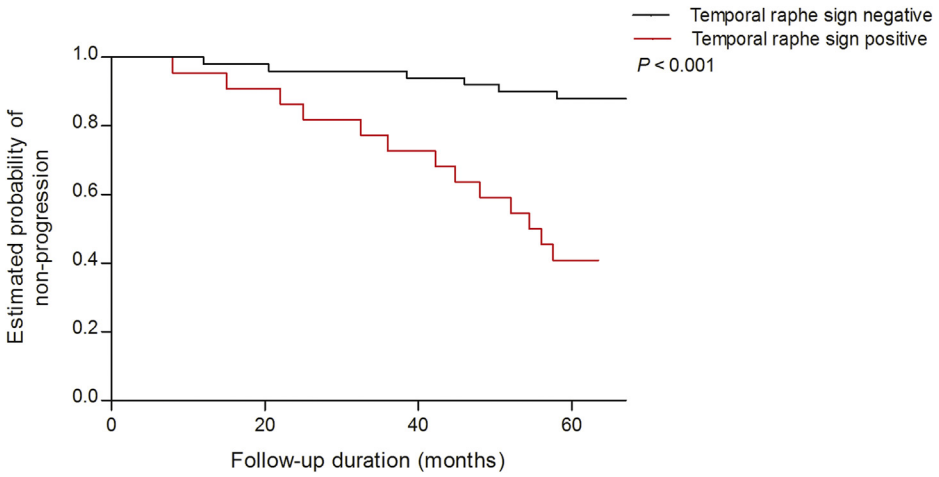

FIGURE 1. Kaplan-Meier curves comparing, among elderly patients with large cup-to-disc ratio (CDR), cumulative probability of normal-tension glaucoma (NTG) conversion. Eyes with temporal raphe sign positivity had a greater cumulative probability of NTG conversion than did those with temporal raphe sign negativity ($P < .001$, log rank test).

also was greater for converters than for nonconverters (-0.40 ± 0.51 vs -0.12 ± 0.45, $P = .028$). The VF location of abnormal points in 7 patients who reached functional endpoints were as follows[34,35]: 5 in superior hemifield (2 early arcuate, 2 arcuate with abnormalities within 5 degrees of fixation, and 1 nasal step) and 2 in inferior hemifield (all early arcuate type).

• **DEMOGRAPHIC AND CLINICAL CHARACTERISTICS OF CONVERTERS AND NONCONVERTERS:** The demographics and baseline clinical characteristics of the 2 groups (converters and nonconverters) are summarized in Table 1. No significant intergroup differences in age, sex distribution, follow-up duration, or systemic factors (eg, diabetes mellitus, systemic hypertension, and cardiopulmonary disease) were found. Likewise, there were no significant differences in IOP factors (ie, baseline, mean, long-term fluctuation, follow-up peak) or in corrected disc area, spherical equivalent, central corneal thickness, or AXL.

Table 2 compares the baseline variables for the 2 groups' RNFL, ONH, ganglion cell analysis, and standard automated perimetry results. The nonconverters' corrected disc area (2.50 ± 0.32 mm^2) was slightly greater than that of the converters (2.47 ± 0.38 mm^2), but not to the point of statistical significance ($P = .090$). The rate of temporal raphe sign positivity was significantly higher among the converters (18 of 19, 94.7%) than among the nonconverters (3 of 53, 5.7%; $P < .001$).

• **COMPARISON OF GLAUCOMA CONVERSION ACCORDING TO PRESENCE OF TEMPORAL RAPHE SIGN:** Among the 72 eyes, the temporal raphe sign was positive in 21 eyes (29.2%). The Kaplan-Meier survival analysis revealed that the eyes with temporal raphe sign positivity had a greater cumulative probability of conversion to glaucoma than did those with temporal raphe sign negativity ($P < .001$; Figure 1). The 5-year survival rate for conversion to glaucoma was 0.41 ± 0.11 for positivity and 0.88 ± 0.05 for negativity ($P < .001$, log rank test).

• **FACTORS ASSOCIATED WITH CONVERSION TO GLAUCOMA IN ELDERLY PATIENTS WITH LARGE CDR:** The multivariate Cox proportional hazards model showed temporal raphe sign positivity to be the factor associated with progression to NTG ($P < .001$). The detailed statistical results, including the hazard ratios and confidence intervals, are available in Table 3.

• **REPRESENTATIVE CASES:** Figure 2 shows representative cases of elderly patients with large CDR. The first column are the results for a male patient (age: 66) with temporal raphe sign positivity at the baseline examination. His baseline IOP was 16 mm Hg. After 5 years of follow-up, focal RNFL defect in the inferotemporal area and a corresponding VF defect had appeared (see the second column). The third and fourth columns are the results for a female patient (age: 68 years) with temporal raphe sign negativity and a baseline IOP of 14 mm Hg. She showed no indications of conversion to NTG during the 5-year follow-up period.

DISCUSSION

THIS STUDY DEMONSTRATED THAT THE PRESENCE OF THE temporal raphe sign on Cirrus SD-OCT's macular GCIPL thickness map is a risk factor for progression to NTG in the elderly with large CDR.

Age-associated RGC loss is already well established. Steady RGC decrement with increasing age has been shown in normal individuals histologically[36–39] as well as

TABLE 3. Univariate and Multivariate Cox Proportional Hazard Models for the Development of Normal-Tension Glaucoma Among Elderly Patients With Large Cup-to-Disc Ratio

	Univariate Model			Multivariate Model		
	HR	95% CI	*P*	HR	95% CI	*P*
Demographic data						
Age (per 1 year older)	1.001	0.914, 1.095	.989			
Sex (male)	0.584	0.235, 1.452	.247			
Diabetes mellitus (yes)	0.881	0.347, 2.237	.789			
Hypertension (yes)	1.000	0.406, 2.460	.999			
Pulmonary disease (yes)	1.110	0.368, 3.347	.852			
Heart disease (yes)	0.842	0.303, 2.337	.741			
Clinical data						
IOP						
Baseline IOP (per 1 mm Hg higher)	1.064	0.852, 1.294	.298			
Mean IOP (per 1 mm Hg higher)	1.087	0.912, 1.296	.351			
IOP fluctuation (per 1 mm Hg higher)	0.636	0.363, 1.114	.114			
Follow-up peak IOP (per 1 mm Hg higher)	1.011	0.847, 1.207	.901			
Axial length (per 1 mm increase)	1.151	0.915, 1.269	.406			
Central corneal thickness (per 1 μm lower)	1.001	0.985, 1.017	.923			
Optic disc hemorrhage (yes)	3.510	0.810, 5.219	.093	2.382	0.538, 5.554	.253
Functional test						
Standard automated perimetry						
MD (per 0.1 dB lower)	0.860	0.650, 1.137	.289			
PSD (per 0.1 dB higher)	1.149	0.360, 3.666	.815			
Number of points with $P < 5\%$ (per point abnormal)	1.080	0.794, 1.469	.624			
Number of points with $P < 1\%$ (per point abnormal)	1.035	0.770, 1.391	.820			
Visual field index (per 1% lower)	0.863	0.571, 1.303	.482			
Structural test						
RNFL and ONH analysis						
RNFL thickness						
Average (per 10 μm thinner)	1.008	0.971, 1.046	.690			
Superior quadrant (per 10 μm thinner)	1.002	0.976, 1.027	.902			
Temporal quadrant (per 10 μm thinner)	1.000	0.898, 1.017	.153			
Inferior quadrant (per 10 μm thinner)	1.022	0.983, 1.020	.860			
Nasal quadrant (per 10 μm thinner)	0.992	0.949, 1.036	.709			
Disc area (per 0.1 mm^2 greater)[a]	0.291	0.073, 1.161	.080	0.742	0.124, 4.448	.744
Average C/D ratio (per 0.1 unit greater)	0.166	0.001, 4.788	.659			
Vertical C/D ratio (per 0.1 unit greater)	0.211	0.001, 1.352	.637			
Cup volume (per 0.1 mm^3 greater)	0.383	0.030, 4.911	.461			
Ganglion cell analysis						
Temporal raphe sign (yes)	6.715	2.538, 17.764	< .001	6.823	2.574, 18.088	< .001
GCIPL thickness						
Average (per 10 μm thinner)	1.020	0.935, 1.113	.656			
Minimum GCIPL thickness (per 10 μm thinner)	1.012	0.948, 1.081	.710			
Superotemporal sector (per 10 μm thinner)	1.055	0.961, 1.159	.259			
Superior sector (per 10 μm thinner)	1.001	0.934, 1.073	.978			
Superonasal sector (per 10 μm thinner)	1.043	0.959, 1.135	.327			
Inferior sector (per 10 μm thinner)	1.021	0.950, 1.098	.573			
Inferotemporal sector (per 10 μm thinner)	1.004	0.948, 1.063	.891			
Inferonasal (per 10 μm thinner)	1.008	0.948, 1.073	.793			

C/D = cup to disc; GCIPL = ganglion cell–inner plexiform layer; HR = hazard ratio; IOP = intraocular pressure; MD = mean deviation; ONH = optic nerve head; PSD = pattern standard deviation; RNFL = retinal nerve fiber layer.

[a]Corrected optic disc area = $3.3822 \times 0.01306^2 \times (\text{axial length-}1.82)^2 \times$ (computed SD-OCT optic disc area).

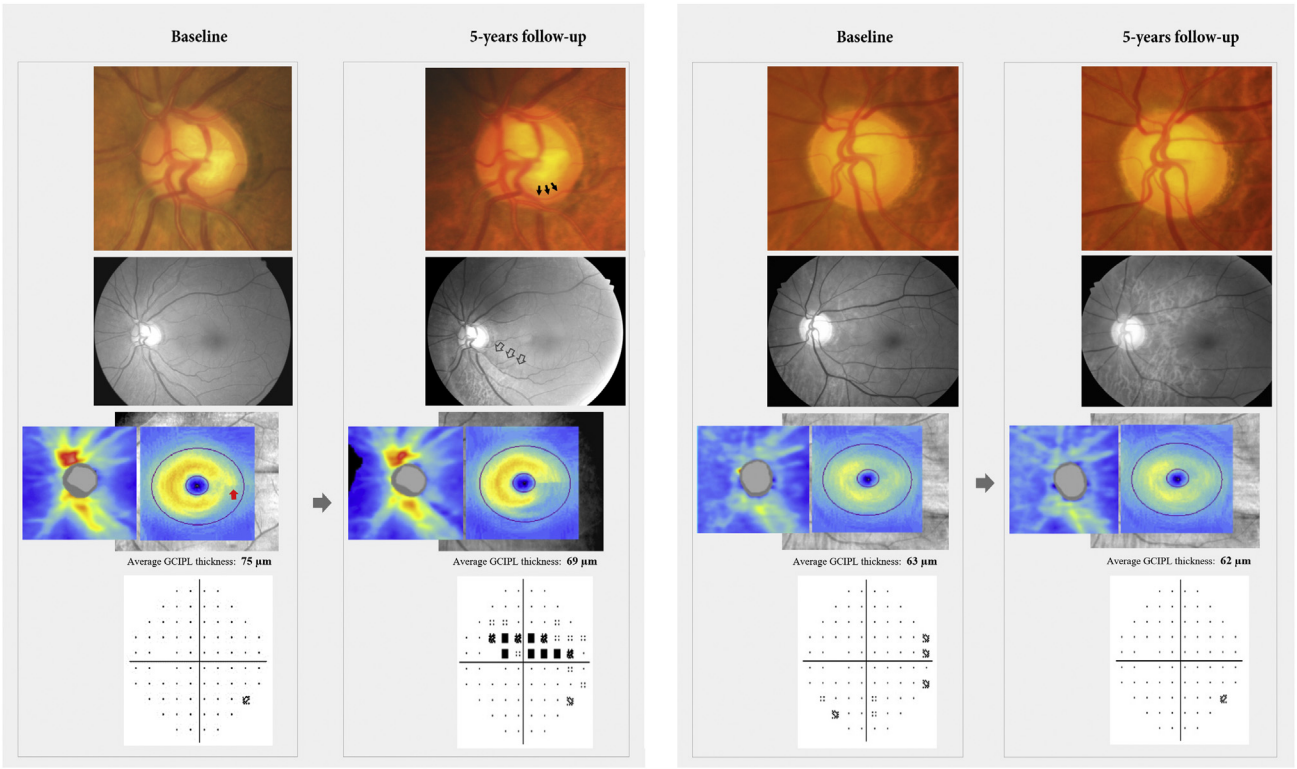

FIGURE 2. Representative cases of elderly patients with large CDR. The first column shows the results for a male patient (age: 66) who had temporal raphe sign positivity at the baseline examination (red arrow). After 5 years of follow-up, further neuroretinal rim narrowing (black arrow), focal RNFL defect in the inferotemporal area (black open arrow), and corresponding VF defect had developed (see the second columns). The figure's third and fourth columns show the results for a female patient (age: 68) who had temporal raphe sign negativity. Significantly, she showed no indications of conversion to NTG during the 5-year follow-up period.

by scanning laser polarimetry[40–42] and OCT.[5–8,43–45] For every 10-year age increase, average RNFL thickness loss ranged from 1.5 to 2.5 µm.[7,45–47] The histologic data also has revealed that approximately 4,000-5,000 optic nerve fibers are lost per year.[2] As life expectancy increases and opportunities for screening examinations are expended, the number of elderly patients diagnosed with glaucoma suspect due to large CDR is expected to grow. In such patients, to determine which cases will go on to progress at rates that exceed age effects is essential, because they can benefit from IOP-lowering treatment.

Although the pathogenesis of glaucoma is still not completely understood, the lamina cribrosa has been known to be the primary site of pathologic change in open-angle glaucoma. The lamina cribrosa's superior and inferior parts seem to have larger pores and thinner connective tissue support for passage of nerve-fiber bundles than do its nasal and temporal parts.[48,49] Such differences have been posited as factors possibly explaining the characteristic early-glaucomatous pattern of damage found in the superotemporal and inferotemporal areas. In previous reports, age-related optic nerve damage showed similar spatial patterns to those of glaucomatous damage.[9–11] It can be deduced that some degree of overlap in biomechanics between optic neuropathy of aging and that of glaucoma in the aged eye might exist.[15] However, the main mechanism of age-associated RGC loss is believed to be increased mitochondrial damage and lost DNA repair capacity, though insults predisposing aged RGCs to injury are likely multiple and various.[50,51] Therefore, it can be expected that age-associated RGC loss exhibits more diffuse change wherein the difference between the superior and inferior hemifields is relatively small.

In early-glaucomatous eyes, macular GCIPL change frequently has been detected prior to any corresponding circumpapillary RNFL change; this probably reflects the GCIPL map's superior sensitivity in allowing for earlier detection of macular-area abnormality.[52] The temporal RNFL, the origins of which respect the horizontal raphe, enters the superotemporal and inferotemporal areas of the optic disc. Because of this segregation, glaucomatous damage is often asymmetric across the horizontal meridian, especially in the early disease stages.[26–28] Meanwhile, age-related loss of GCIPL has shown a more spatially homogenous pattern across sectors.[53] Thus, GCIPL thickness could be better suited to assessment of the progression of

structural glaucomatous loss. Indeed, temporal raphe sign positivity, which reflects asymmetric GCIPL damage across the horizontal raphe, showed a great utility for evaluation of risk of NTG conversion in the present study. The temporal raphe sign has been suggested as an effective practical indicator for evaluation of the probability of glaucomatous damage, despite the absence of any computer program.[30] That is, this sign can be a simple but directly applicable clinical tool for discriminating elderly glaucoma suspects with higher risk of further progression.

There have been many studies investigating differences between retinal hemispheres in macular thickness as an indicator of early glaucomatous damage.[25–27,54,55] However, it has not been determined whether the significance of such asymmetry differs between NTG and glaucoma with higher baseline pressure. It has been previously reported that glaucomatous damages are deeper and closer to fixation in NTG as compared with high-pressure-glaucoma eyes.[56] Longitudinal structural change in patients with lower pretreatment IOP tends to be detected on the macular GCIPL before peripapillary RNFL.[57] In our cohort, all of the enrolled subjects were East Asian (Korean) with untreated IOP ≤21 mm Hg. Our results therefore might not be directly applicable to other ethnic groups or glaucoma patients with higher baseline IOP. In addition, it remains important to consider the possibility of nonconverters developing glaucoma over extended periods of time. However, in the present study, the mean age of the nonconverter group was 77.8 years at the final visit, and there were still no indications of glaucomatous change after an average 5.4 years of follow-up. Considering that the life expectancy of the race of patients (Korean) participating in our study was 82,[58] even if they eventually reached endpoints for NTG, it would be less likely to significantly affect their quality of life.

Even though temporal raphe sign positivity well predicted conversion to NTG, there were some misclassification cases. Notably, in the 4 misclassified cases (1 showed NTG conversion with absence of baseline temporal raphe sign and 3 had a positive temporal raphe sign but did not reach the endpoints for NTG), the patient showed NTG conversion but baseline temporal raphe sign negativity, had superotemporal RNFL defect with a large angular distance from the macula. It is known that macular GCIPL parameters are less sensitive in cases where the temporal margin of the defect is located far from the fovea.[59] Thus, this factor should be given due consideration when determining temporal raphe sign presence or absence and when assessing early-glaucomatous damage in elderly patients showing large CDR.

An important goal of our study was to establish a clinical feature that could facilitate clinicians' determination of elderly patients who need closer monitoring in real clinical practice. Although detailed quantitative analysis by OCT certainly will give much more information on suspicious ONH, it might often prove difficult to apply in daily practice. Thus, we focused our analysis on clinical disc examination for patient inclusion and OCT parameters that can be directly obtained from OCT images for outcome criteria. To improve diagnostic precision on glaucoma suspects, however, the importance of quantitative evaluation for structural abnormality by OCT imaging should not be overlooked.[60–62] Additionally, considering clinician variability in clinical disc examination,[63,64] the importance of quantitatively detecting structural abnormality by OCT imaging should be better emphasized. Application of the newly proposed OCT parameters and combined-parameter indices as well as analysis of how they can improve diagnostic accuracy in elderly glaucoma suspects certainly deserve further study.

The following points must be considered when interpreting the present study's results. First, its retrospective design has inherent possible biases. A future prospective, longitudinal study investigating baseline predictors of progression at rates exceeding age effects is warranted. Second, we did not distinguish eyes satisfying only 1 or 2 of the 3 conditions for the temporal raphe sign. We believe that application of algorithms that can identify "partial" or "incomplete" temporal raphe sign as well as analyze how they can affect diagnostic accuracy in glaucoma suspects deserves further study. Third, this study included patients who had been visiting a clinic every 6 months; thus, it was possible that patients of higher socioeconomic status and/or better general medical condition were selectively included in the study. Finally, although a large CDR had been used as a sign of possible glaucomatous damage, CDR depends on optic disc size.[65] However, because there was no significant difference in AXL-adjusted disc area between the nonconverter and converter groups, optic disc area was less likely to be a significant confounding factor in the current study.

In conclusion, temporal raphe sign positivity on the baseline macular GCIPL thickness map was associated with higher risk of NTG conversion in elderly subjects with large CDR. In clinical practice, therefore, temporal raphe sign on OCT macular scans can facilitate the determination of cases that need more vigilant monitoring for future structural or functional progression in elderly patients with large CDR.

FUNDING/SUPPORT: THIS STUDY RECEIVED NO FUNDING. FINANCIAL DISCLOSURES: THE AUTHORS INDICATE NO FINANCIAL support or conflicts of interest. All authors attest that they meet the current ICMJE criteria for authorship.

REFERENCES

1. Gao H, Hollyfield J. Aging of the human retina. Differential loss of neurons and retinal pigment epithelial cells. *Invest Ophthalmol Vis Sci* 1992;33(1):1–17.
2. Jonas JB, Schmidt AM, Muller-Bergh JA, Schlotzer-Schrehardt UM, Naumann GO. Human optic nerve fiber count and optic disc size. *Invest Ophthalmol Vis Sci* 1992; 33(6):2012–2018.
3. Repka MX, Quigley HA. The effect of age on normal human optic nerve fiber number and diameter. *Ophthalmology* 1989; 96(1):26–32.
4. Demirkaya N, van Dijk HW, van Schuppen SM, et al. Effect of age on individual retinal layer thickness in normal eyes as measured with spectral-domain optical coherence tomography. *Invest Ophthalmol Vis Sci* 2013;54(7):4934–4940.
5. Patel NB, Lim M, Gajjar A, Evans KB, Harwerth RS. Age-associated changes in the retinal nerve fiber layer and optic nerve head. *Invest Ophthalmol Vis Sci* 2014;55:5134–5143.
6. Zhang X, Francis BA, Dastiridou A, et al. Longitudinal and cross-sectional analyses of age effects on retinal nerve fiber layer and ganglion cell complex thickness by Fourier-domain OCT. *Transl Vis Sci Technol* 2016;5(2):1.
7. Parikh RS, Parikh SR, Sekhar GC, Prabakaran S, Babu JG, Thomas R. Normal age-related decay of retinal nerve fiber layer thickness. *Ophthalmology* 2007;114(5):921–926.
8. Leung CK, Yu M, Weinreb RN, et al. Retinal nerve fiber layer imaging with spectral-domain optical coherence tomography: a prospective analysis of age-related loss. *Ophthalmology* 2012; 119(4):731–737.
9. See JL, Nicolela MT, Chauhan BC. Rates of neuroretinal rim and peripapillary atrophy area change: a comparative study of glaucoma patients and normal controls. *Ophthalmology* 2009; 116(5):840–847.
10. Burgoyne CF. A biomechanical paradigm for axonal insult within the optic nerve head in aging and glaucoma. *Exp Eye Res* 2011;93(2):120–132.
11. Vianna JR, Danthurebandara VM, Sharpe GP, et al. Importance of normal aging in estimating the rate of glaucomatous neuroretinal rim and retinal nerve fiber layer loss. *Ophthalmology* 2015;122(12):2392–2398.
12. Chauhan BC, Danthurebandara VM, Sharpe GP, et al. Bruch's membrane opening minimum rim width and retinal nerve fiber layer thickness in a normal white population: a multicenter study. *Ophthalmology* 2015;122:1786–1794.
13. Zangalli CS, Vianna JR, Reis AS, et al. Bruch's membrane opening minimum rim width and retinal nerve fiber layer thickness in a Brazilian population of healthy subjects. *PLoS One* 2018;13(12):e0206887.
14. Araie M, Iwase A, Sugiyama K, et al. Determinants and characteristics of Bruch's membrane opening and Bruch's membrane opening–minimum rim width in a normal Japanese population. *Invest Ophthalmol Vis Sci* 2017;58(10): 4106–4113.
15. Burgoyne CF, Downs JC. Premise and prediction–how optic nerve head biomechanics underlies the susceptibility and clinical behavior of the aged optic nerve head. *J Glaucoma* 2008;17(4):318.
16. Albon J, Karwatowski WS, Easty DL, et al. Age related changes in the non-collagenous components of the extracellular matrix of the human lamina cribrosa. *Br J Ophthalmol* 2000;84(3):311–317.
17. Quigley HA. Childhood glaucoma: results with trabeculotomy and study of reversible cupping. *Ophthalmology* 1982; 89(3):219–226.
18. Morrison JC, Jerdan JA, Dorman ME, Quigley HA. Structural proteins of the neonatal and adult lamina cribrosa. *Arch Ophthalmol* 1989;107(8):1220–1224.
19. Fazio P, Krupin T, Feitl ME, et al. Optic disc topography in patients with low-tension and primary open angle glaucoma. *Arch Ophthalmol* 1990;108(5):705–708.
20. Sowka J. New thoughts on normal tension glaucoma. *J Am Optom Assoc* 2005;76(10):600–608.
21. Curcio CA, Saunders PL, Younger PW, et al. Peripapillary chorioretinal atrophy: Bruch's membrane changes and photoreceptor loss. *Ophthalmology* 2000;107(2):334–343.
22. Jonas J, Naumann G. Parapapillary chorioretinal atrophy in normal and glaucoma eyes. II. Correlations. *Invest Ophthalmol Vis Sci* 1989;30(5):919–926.
23. Park KH, Tomita G, Liou SY, et al. Correlation between peripapillary atrophy and optic nerve damage in normal-tension glaucoma. *Ophthalmology* 1996;103(11):1899–1906.
24. Bak E, Ha A, Kim YW, et al. Ten-year-and-beyond longitudinal change of ß-zone parapapillary atrophy: comparison of primary open-angle glaucoma with normal eyes. *Ophthalmology* 2020;127(8):1054–1063.
25. Asrani S, Rosdahl JA, Allingham RR. Novel software strategy for glaucoma diagnosis: asymmetry analysis of retinal thickness. *Arch Ophthalmol* 2011;129(9):1205–1211.
26. Um TW, Sung KR, Wollstein G, et al. Asymmetry in hemifield macular thickness as an early indicator of glaucomatous change. *Invest Ophthalmol Vis Sci* 2012;53(3):1139–1144.
27. Yamada H, Hangai M, Nakano N, et al. Asymmetry analysis of macular inner retinal layers for glaucoma diagnosis. *Am J Ophthalmol* 2014;158(6):1318–1329.e3.
28. Kim YK, Yoo BW, Kim HC, Park KH. Automated detection of hemifield difference across horizontal raphe on ganglion cell–inner plexiform layer thickness map. *Ophthalmology* 2015;122(11):2252–2260.
29. Kim YK, Yoo BW, Jeoung JW, Kim HC, Kim HJ, Park KH. Glaucoma-diagnostic ability of ganglion cell-inner plexiform layer thickness difference across temporal raphe in highly myopic eyes. *Invest Ophthalmol Vis Sci* 2016;57(14):5856–5863.
30. Lee J, Kim YK, Ha A, et al. Temporal raphe sign for discrimination of glaucoma from optic neuropathy in eyes with macular ganglion cell-inner plexiform layer thinning. *Ophthalmology* 2019;126(8):1131–1139.
31. Moghimi S, Hosseini H, Riddle J, et al. Measurement of optic disc size and rim area with spectral-domain OCT and scanning laser ophthalmoscopy. *Invest Ophthalmol Vis Sci* 2012; 53(8):4519–4530.
32. Bennett AG, Rudnicka AR, Edgar DF. Improvements on Littmann's method of determining the size of retinal features by fundus photography. *Graefes Arch Clin Exp Ophthalmol* 1994;232(6):361–367.
33. Kim YK, Park KH, Yoo BW, Kim HC. Topographic characteristics of optic disc hemorrhage in primary open-angle glaucoma. *Invest Ophthalmol Vis Sci* 2014;55(1):169–176.
34. Fellman R, Mattox C, Ross K, et al. Know the new glaucoma staging codes. *EyeNet* 2011;10:65Y66.

35. Ding X, Chang RT, Guo X, et al. Visual field defect classification in the Zhongshan Ophthalmic Center–Brien Holden Vision Institute High Myopia Registry Study. *Br J Ophthalmol* 2016;100(12):1697–1702.
36. Dolman CL, McCormick AQ, Drance SM. Aging of the optic nerve. *Arch Ophthalmol* 1980;98(11):2053–2058.
37. Balazsi A, Rootman J, Drance S, Schulzer M, Douglas G. The effect of age on the nerve fiber population of the human optic nerve. *Am J Ophthalmol* 1984;97(6):760–766.
38. Johnson BM, Miao M, Sadun AA. Age-related decline of human optic nerve axon populations. *Age* 1987;10(1):5–9.
39. Jonas JB, Müller-Bergh J, Schlötzer-Schrehardt U, Naumann G. Histomorphometry of the human optic nerve. *Invest Ophthalmol Vis Sci* 1990;31(4):736–744.
40. Tjon-Fo-Sang MJ, DE Vries J, Lemij HG. Measurement by nerve fiber analyzer of retinal nerve fiber layer thickness in normal subjects and patients with ocular hypertension. *Am J Ophthalmol* 1996;122(2):220–227.
41. Poinoosawmy D, Fontana L, Wu J, Fitzke F, Hitchings R. Variation of nerve fibre layer thickness measurements with age and ethnicity by scanning laser polarimetry. *Br J Ophthalmol* 1997;81(5):350–354.
42. Da Pozzo S, Iacono P, Marchesan R, Minutola D, Ravalico G. The effect of ageing on retinal nerve fibre layer thickness: an evaluation by scanning laser polarimetry with variable corneal compensation. *Acta Ophthalmol Scand* 2006;84(3):375–379.
43. Schuman JS, Hee MR, Puliafito CA, et al. Quantification of nerve fiber layer thickness in normal and glaucomatous eyes using optical coherence tomography: a pilot study. *Arch Ophthalmol* 1995;113(5):586–596.
44. Varma R, Bazzaz S, Lai M. Optical tomography–measured retinal nerve fiber layer thickness in normal Latinos. *Invest Ophthalmol Vis Sci* 2003;44(8):3369–3373.
45. Budenz DL, Anderson DR, Varma R, et al. Determinants of normal retinal nerve fiber layer thickness measured by Stratus OCT. *Ophthalmology* 2007;114(6):1046–1052.
46. Bendschneider D, Tornow RP, Horn FK, et al. Retinal nerve fiber layer thickness in normals measured by spectral domain OCT. *J Glaucoma* 2010;19(7):475–482.
47. Feuer WJ, Budenz DL, Anderson DR, et al. Topographic differences in the age-related changes in the retinal nerve fiber layer of normal eyes measured by Stratus optical coherence tomography. *J Glaucoma* 2011;20(3):133–138.
48. Jonas JB, Mardin CY, Schlotzer-Schrehardt U, Naumann GO. Morphometry of the human lamina cribrosa surface. *Invest Ophthalmol Vis Sci* 1991;32(2):401–405.
49. Quigley HA, Addicks EM. Regional differences in the structure of the lamina cribrosa and their relation to glaucomatous optic nerve damage. *Arch Ophthalmol* 1981;99(1):137–143.
50. Wang AL, Lukas TJ, Yuan M, Neufeld AH. Age-related increase in mitochondrial DNA damage and loss of DNA repair capacity in the neural retina. *Neurobiol Aging* 2010;31(11):2002–2010.
51. Chrysostomou V, Trounce IA, Crowston JG. Mechanisms of retinal ganglion cell injury in aging and glaucoma. *Ophthalmic Res* 2010;44(3):173–178.
52. Kim YK, Ha A, Na KI, et al. Temporal relation between macular ganglion cell–inner plexiform layer loss and peripapillary retinal nerve fiber layer loss in glaucoma. *Ophthalmology* 2017;124(7):1056–1064.
53. Chauhan BC, Vianna JR, Sharpe GP, et al. Differential effects of aging in the macular retinal layers, neuroretinal rim, and peripapillary retinal nerve fiber layer. *Ophthalmology* 2020;127(2):177–185.
54. Bagga H, Greenfield DS, Knighton RW. Macular symmetry testing for glaucoma detection. *J Glaucoma* 2005;14(5):358–363.
55. Hwang YH, Ahn SI, Ko SJ. Diagnostic ability of macular ganglion cell asymmetry for glaucoma. *Clin Exp Ophthalmol* 2015;43(8):720–726.
56. Ahrlich KG, De Moraes CGV, Teng CC, et al. Visual field progression differences between normal-tension and exfoliative high-tension glaucoma. *Invest Ophthalmol Vis Sci* 2010;51(3):1458–1463.
57. Marshall HN, Andrew NH, Hassall M, et al. Macular ganglion cell–inner plexiform layer loss precedes peripapillary retinal nerve fiber layer loss in glaucoma with lower intraocular pressure. *Ophthalmology* 2019;126(8):1119–1130.
58. World Health Organization. World Health Statistics 2016: Monitoring Health for the SDGs. Geneva: WHO Press; 2016.
59. Kim MJ, Jeoung JW, Park KH, et al. Topographic profiles of retinal nerve fiber layer defects affect the diagnostic performance of macular scans in preperimetric glaucoma. *Invest Ophthalmol Vis Sci* 2014;55(4):2079–2087.
60. Yang H, Luo H, Hardin C, et al. OCT structural abnormality detection in glaucoma using topographically correspondent rim and retinal nerve fiber layer criteria. *Am J Ophthalmol* 2020;213:203–216.
61. Gmeiner JM, Schrems WA, Mardin CY, et al. Comparison of Bruch's membrane opening minimum rim width and peripapillary retinal nerve fiber layer thickness in early glaucoma assessment. *Invest Ophthalmol Vis Sci* 2016;57(9):OCT575–OCT584.
62. Park K, Kim J, Lee J. The relationship between bruch's membrane opening-minimum rim width and retinal nerve fiber layer thickness and a new index using a neural network. *Transl Vis Sci Technol* 2018;7(4):14.
63. Hong SW, Koenigsman H, Ren R, et al. Glaucoma specialist optic disc margin, rim margin, and rim width discordance in glaucoma and glaucoma suspect eyes. *Am J Ophthalmol* 2018;192:65–76.
64. Hong SW, Koenigsman H, Yang H, et al. Glaucoma specialist detection of optical coherence tomography suspicious rim tissue in glaucoma and glaucoma suspect eyes. *Am J Ophthalmol* 2019;199:28–43.
65. Heijl A, Molder H. Optic disc diameter influences the ability to detect glaucomatous disc damage. *Acta Ophthalmol* 1993;71(1):122–129.